NASA Technical Memorandum 106013
AIAA–93–0147

Propagation of High Frequency Jet Noise Using Geometric Acoustics

A. Khavaran
Sverdrup Technology, Inc.
Lewis Research Center Group
Brook Park, Ohio

and

E.A. Krejsa
National Aeronautics and Space Administration
Lewis Research Center
Cleveland, Ohio

Prepared for the
31st Aerospace Sciences Meeting and Exhibit
sponsored by the American Institute of Aeronautics and Astronautics
Reno, Nevada, January 11–14, 1993

NASA

Propagation of High Frequency Jet Noise Using Geometric Acoustics

A. Khavaran *
Sverdrup Technology, Inc.
NASA Lewis Research Center
Cleveland, OH 44135

E.A. Krejsa*
NASA Lewis Research Center
Cleveland, OH 44135

Abstract

Spherical directivity of noise radiated from a convecting quadrupole source embedded in an arbitrary spreading jet is obtained by ray-tracing methods of geometrical acoustics. The six propagation equations are solved in their general form in a rectangular coordinate system. The noise directivity in the far field is calculated by applying an iteration scheme that finds the required radiation angles at the source resulting in propagation through a given observer point. Factors influencing the zone of silence are investigated. The caustics of geometrical acoustics and the exact location where it forms is demonstrated by studying the variation in ray tube area obtained from transport equation. For a ring source convecting along the center-axis of an axisymmetric jet, the polar directivity of the radiated noise is obtained by an integration with respect to azimuthal directivity of compact quadrupole sources distributed on the ring. The Doppler factor is shown to vary slightly from point to point on the ring. Finally the scaling of the directivity pattern with power -3 of Doppler factor is investigated and compared with experimental data.

Introduction

The study of aerodynamic noise has its foundation in Lighthill's acoustic analogy. By defining the source term in his theory of aerodynamic sound generation, he opened the door to a vast scientific knowledge already developed in theoretical acoustics. Besides the generation aspects of the sound which have been extensively researched in the past [1, 2], the propagation through moving fluids is an important aspect of jet noise computation. When we compare the acoustic wavelength with the characteristic length of the flow, within the three-way subdivision, two are relatively easier. The easier cases, as noted by Lighthill [3], correspond to situations when the emitted wave has a wavelength much shorter or much longer than the characteristic length of the flow. The high frequency solution appears to provide a reasonably good approximation even at Helmholtz numbers as small as one [4, 5, 6], and is of particular interest in prediction of noise directivity for high speed jets.

A number of investigators have studied the radiation field of multipole sources immersed in parallel sheared flows. Gliebe and Balsa [7] and Goldstein [8] studied the sound/flow interaction for round jets with arbitrary velocity profiles assuming quadrupole sources convecting along the centerline in both high and low frequency limits, respectively. The generalization to arbitrarily located sources in continuously varying monotonic profiles were derived by Balsa [9] and Goldstein [10, 11]. For a parallel flow study, Lilley's equation is considered as the starting point by most investigators studying the sound/flow interaction. For axisymmetric jets, the Green's function solution to a convected monopole of frequency ω is obtained by applying a sequence of Fourier transformations. The solution for multipole singularities is derived by differentiating the monopole solution with respect to appropriate source coordinates. Mani, Gliebe and Balsa [12] provide a comprehensive analysis of the shielding effects of parallel jets when velocity and temperature profiles are functions of the radial variable only. Their derivation was used by the present authors in the computation of supersonic jet mixing noise of a CD nozzle [13]. Schubert [14, 15] computes the directivity pattern of a harmonic point source on the axis of a subsonic jet flow with a carefully selected velocity profile. He compares the ray acoustic solution with the wave acoustic predictions based on the finite difference solution to convected wave equation. He concludes that the presence of downstream zone of silence is primarily due to refraction rather than an inherent characteristic of turbulence generated noise. His computations show that the geometric acoustics solution predicts an axial refraction valley much deeper than the observation and he argues that this difference is due to the diffraction

* Member, AIAA.

effect at lower frequencies which is missing in a ray acoustic prediction.

To study the effect of asymmetry in the mean flow, Goldstein [16] solves Lilley's equation for high frequency multipole sources in a parallel jet flow whose Mach number and temperature are functions of the cross-flow coordinates. In the high frequency limit one can recover equations similar to those governing the two-dimensional waves generated by a line source in a non-moving medium with variable index of refraction. Avila and Keller [17] solved this problem using matched asymptotic expansions. The corresponding sound field directivity is determined by solving a fourth order ordinary differential equation which finds the projection of rays on a cross-flow plane. This solution technique, though successful in giving a qualitative picture of circumferential directivity of jet noise for non-axisymmetric plumes, fails near the zone of silence. Within the boundary of the zone of silence of a source, the acoustic rays get trapped in an envelope that prevents the radiation to the far field.

Thus, a full three-dimensional ray-tracing approach becomes necessary where one can study the refraction of acoustic rays as they emerge from the source on their way to a distant observer. This solution technique provides the tools for investigating the zone of silence as well as the caustics of geometrical acoustics.

A high frequency Green function for a convecting multipole source in a spreading jet was developed by P. A. Durbin [18] and was applied to predict the directivity of noise for a source convecting along the center-axis of an axisymmetric jet. The symmetric nature of this problem, confines the acoustic rays to a constant azimuthal plane and thus, reduces the number of propagation equations from six to two. Following the methodology described by Durbin [18, 19], an attempt has been made here to predict the spherical directivity of a convecting quadrupole source in an arbitrary flow. The six propagation equations are solved in a rectangular coordinate system. As we shall describe under numerical results, the solution to the corresponding boundary value problem based on specified source and observer locations, requires an iteration on the initial ray angles. The jet spreading as well as plume profile strongly influence the size of the zone of silence. The jet spreading does not necessarily remove the zone of silence; rather velocity gradients near the center-axis have a dominant role in defining the boundary of the zone of silence. The neighbourhood of the caustic is described by studying the variation in ray tube area obtained from the transport equation. It should be emphasized that the flow gradients should be small for the geometric ray theory to work. For cases when shocks are present, special treatment will be necessary to properly trace the rays across a discontinuity. In addition, no attempt has been made here to derive expressions valid near the caustic, although solutions similar to those derived for a still medium can be expected [20, 21, 22].

Governing Equations

The relevant equations are the linearized gasdynamic equations governing the propagation of small disturbances through a steady mean flow. For a source with time harmonic factor $e^{-i\omega t}$ the inhomogeneous equations of continuity and momentum are

$$-i\omega\rho' + \nabla\cdot(\mathbf{U}\rho' + \mathbf{u}\rho) = a^2 Q_d$$

$$-i\omega\mathbf{u} + \mathbf{U}\cdot\nabla\mathbf{u} + \mathbf{u}\cdot\nabla\mathbf{U} + \nabla(a^2\rho'/\rho) = -(a^2/\rho)\mathbf{Q}_m \quad (1)$$

where ρ' and $\mathbf{u}$ are the density and velocity of the acoustic fluctuations and ρ and $\mathbf{U}$ are the corresponding quantities for the mean flow, a is the mean flow sound speed and Q_d and $\mathbf{Q}_m$ represent the source terms. In a region not close to the source, the amplitude variation of the acoustic disturbances is slow and a high frequency solution to the homogeneous form of equations (1) can be found by substituting the classical expansions in inverse powers of the wave number $k = \omega/a_r$:

$$\rho' = \{\varrho + (1/ik)\varrho_1 + \cdots\}\, e^{ikL(\mathbf{X})}$$
$$\mathbf{u} = \{\mathbf{v} + (1/ik)\mathbf{v_1} + \cdots\}\, e^{ikL(\mathbf{X})} \quad (2)$$

where a_r is a typical reference sound speed. Factoring the coefficients of equal powers of k and setting each factor equal to zero independently, one can find a series of equations describing the behavior of wave fronts of constant phase and equations for transport of energy. The first of such equations is eikonal equation. It describes the change in the normal to the phase front due to refraction caused by nonuniformities in the flow velocity and temperature. Introducing the normal to the phase front as $\mathbf{p} = \nabla L$, and Mach number $\mathbf{M} = \mathbf{U}/a$ and dimensionless sound speed $C(\mathbf{X}) = a/a_r$, the eikonal equation is expressed as

$$(M_i p_i - 1/C)^2 = p_i p_i. \quad (3)$$

The rays generated by the eikonal equation are solved by the method of characteristics. Thus, along the ray $\mathbf{X}(t)$ and $\mathbf{p}(t)$ can be calculated by solving a system of six ordinary differential equations [18, 23]:

$$\dot{X}_i = T_{ij}p_j + M_i/C \quad (4)$$

$$\dot{p}_i = -\frac{1}{2}p_j\frac{\partial T_{jk}}{\partial X_i}p_k - p_j\frac{\partial}{\partial X_i}\left(\frac{M_j}{C}\right) + \frac{1}{2}\frac{\partial}{\partial X_i}(C^{-2}). \quad (5)$$

Tensor T_{ij} is related to Mach number $\mathbf{M}$; ($T_{ij} = \delta_{ij} - M_i M_j$). The initial conditions for equations (4) and (5) are the source location $\mathbf{X} = \mathbf{X}_o$ and the direction at which the ray leaves the source. Along the ray, velocity $\dot{\mathbf{X}}$ can be expressed in terms of unit vector $\hat{\mathbf{X}}$ and ray speed $\lambda = \mid \dot{\mathbf{X}} \mid$ as $\dot{\mathbf{X}} = \lambda \hat{\mathbf{X}}$. Substituting $\dot{\mathbf{X}}$ in (4) and solving equations (3) and (4) simultaneously, one can find $\mathbf{p}$ as

$$\mathbf{p} = \lambda \hat{\mathbf{X}} + (\lambda \hat{\mathbf{X}} \cdot \mathbf{M} - \frac{1}{C}) \frac{\mathbf{M}}{\beta^2} \tag{6}$$

$$\lambda = [\beta^2 + (\hat{\mathbf{X}} \cdot \mathbf{M})^2]^{-\frac{1}{2}} / C \tag{7}$$

where $\beta^2 = 1 - \mid \mathbf{M} \mid^2$. When the source is placed at the vertex of a cone of semiangle μ with axis parallel to X (referred to as cone of emission), each ray can be defined along the generator of the cone through angle δ (figure 1). Along such a ray the initial direction can be expressed through unit vector $\hat{\mathbf{X}}_o = (cos\,\mu,\ sin\,\mu\, cos\,\delta,\ sin\,\mu\, sin\,\delta)$. The corresponding phase normal $\mathbf{p}_o$ is given by (6) and (7) provided that ${\beta_o}^2 \neq 0$; where subscript o applies to the source location. When the source Mach number equals one, it can be concluded from (6) and (7) that

$$\mathbf{p}_o = (\hat{\mathbf{X}}_o - \frac{.5\mathbf{M}_o}{\hat{\mathbf{X}}_o \cdot \mathbf{M}_o}) / (C_o \hat{\mathbf{X}}_o \cdot \mathbf{M}_o), \qquad \mid \mathbf{M}_o \mid = 1. \tag{8}$$

Now when the flow becomes supersonic, the ray speed λ_o as given by (7) is real only if

$$1 - \mid \mathbf{M}_o \mid^2 + (\hat{\mathbf{X}}_o \cdot \mathbf{M}_o)^2 \geq 0. \tag{9}$$

It can be shown that this condition is always true provided that the limit value on the direction of emission at the source is imposed. If χ is the angle between the Mach vector and $\hat{\mathbf{X}}$ and ψ is the corresponding angle between the Mach vector and the phase normal $\mathbf{p}$ one can show that along the ray $\mid \mathbf{M} \mid sin\,\chi = sin\,(\psi - \chi)$. At the source this relation translates into $\mid \mathbf{M}_o \mid sin\,\chi_o = sin\,(\psi_o - \chi_o) \leq 1$ which guarantees that (9) is always satisfied. As the jet Mach number increases , angle χ_o should decrease accordingly for $\mid \mathbf{M}_o \mid sin\,\chi_o \leq 1$, resulting in a reduction in the limit value for the cone angle μ.

The transport equation, obtained from the next order of k in the governing equations, can be simplified as

$$\nabla \cdot (\rho \dot{\mathbf{X}} \Gamma^2) = 0, \qquad \Gamma = \frac{(\varrho/\rho)}{\frac{1}{C} - \mathbf{M} \cdot \mathbf{p}}. \tag{10}$$

Equation (10) leads to the wave action conservation equation [24] which states that the action contained in a wave packet is invariant along each characteristic line

$$\lambda \Gamma^2 \rho J = constant \tag{11}$$

where J measures the variation of the ray tube cross-section along each ray. The variation in the ray tube area can be expressed in terms of a transformation which maps the initial ray angles (μ, δ) onto the final direction at the observer location (r, θ_∞, ϕ_∞). Assuming that in the far field the rays become straight, it can easily be shown that

$$J = r^2\, sin\,\theta_\infty \mid \frac{\partial(\theta_\infty, \phi_\infty)}{\partial(\mu, \delta)} \mid . \tag{12}$$

Thus, the field amplitude ϱ is obtained from equation (11) once the elemental wave front area J has been determined. To find the constant in equation (11), an appropriate near source solution satisfying (1) is asymptotically matched with the outer solution. The details of the analysis are spelled out in [18] and are not repeated here. If a_r is taken to be the stagnation sound speed a_∞, the first term in the high frequency approximation for equation (2) is

$$\rho' \propto \varrho\, e^{ikL} = (\frac{1}{4\pi r})(\frac{C_o}{C}) \frac{1 - \frac{\mathbf{U}}{a_\infty} \cdot \mathbf{p}}{1 - \frac{\mathbf{U}_a}{a_\infty} \cdot \mathbf{p}_o} \times$$

$$\left\{ \frac{\rho}{\rho_o} \frac{\lambda_o^3}{\lambda} \frac{sin\,\mu}{sin\,\theta_\infty} \frac{{C_o}^2}{\mid \frac{\partial(\theta_\infty, \phi_\infty)}{\partial(\mu, \delta)} \mid} \right\}^{1/2} e^{ikL}. \tag{13}$$

This Green function can be used to derive an expression for the mean square pressure for a convecting quadrupole source [16, 18]. In the high frequency approximation the source frequency ω_o can be related to the observer frequency ω through the Doppler factor

$$\omega = \omega_o / (1 - \frac{\mathbf{U}_c}{a_\infty} \cdot \mathbf{p}_o) \tag{14}$$

where $\mathbf{U}_c$ is the source convection velocity.

If the spectral power intensity for the source is represented as $\overline{\mid \hat{Q}(\omega_o) \mid^2}$, the source power within a narrow-band $\Delta\omega_o$ is ${Q_o}^2 = \overline{\mid \hat{Q}(\omega_o) \mid^2} \Delta\omega_o$. The resulting mean-square pressure directivity for a convecting isotropic quadrupole is given as

$$\overline{P^2}(\omega, \mathbf{X}) \propto (\frac{1}{4\pi r})^2 {\omega_o}^4 Q_o^2 (\frac{\rho}{\rho_o})(\frac{\lambda_o^3}{\lambda})(\frac{sin\,\mu}{sin\,\theta_\infty}) \times$$

$$\frac{(1 - \frac{\mathbf{U}_a}{a_\infty} \cdot \mathbf{p}_o)^2 (1 - \frac{\mathbf{U}}{a_\infty} \cdot \mathbf{p})^2}{(1 - \frac{\mathbf{U}_c}{a_\infty} \cdot \mathbf{p}_o)^5 \mid \frac{\partial(\theta_\infty, \phi_\infty)}{\partial(\mu, \delta)} \mid}. \tag{15}$$

It can be seen from (14) that the source frequency should be different from point to point in order for a

fixed observer to hear the same frequency. This is essentially due to refraction phenomena resulting in variation of $\mathbf{p_o}$ for each ray reaching a given observer and will be explored later by computing the Doppler factor for source points distributed around the axis of an axisymmetric jet. It is also important to remember that for the purpose of numerical computation of equation (15), no attempt has been made to specify the source strength. Determination of the source correlation term and its spectrum, by itself, is a major area of research in computational aeroacoustics. An approach based on computation of turbulence kinetic energy and its dissipation rate using CFD is described in [13].

Velocity and Temperature Profiles

In order to integrate the propagation equations, the jet velocity and sound speed are expressed in a closed form to speed up the computation of derivatives. For a jet spreading at angle α, a self-similar velocity profile with appropriate decay characteristics can be expressed as

$$\mathbf{U}(r,\theta)/a = (\mathbf{U}/a)_{CL}\, e^{-(\frac{r}{a})^n} \qquad (16)$$

where $(\mathbf{U}/a)_{CL}$ is the Mach number on the centerline and θ is the polar angle defined earlier. The velocity decay on the center-axis of the jet has been measured experimentally for different nozzle geometries and exit conditions. For a convergent nozzle, the peak Mach can be expressed as a function of axial distance parameter L_x [25]

$$(\mathbf{U}/a_\infty)_{CL} = (\mathbf{U_j}/a_\infty)\left\{1+(.15L_x)^4\right\}^{-.25}$$

$$L_x = \frac{X/D}{C_n\sqrt{1+M_j}}. \qquad (17)$$

The jet exit Mach number $M_j = U_j/a_\infty$ can vary in a relatively wide range and $C_n = .82$. D is the exit diameter and X is measured from exit plane (figure 1). Using the adiabatic flow relation combined with equations (16) and (17), the Mach number and sound speed are given as

$$M = \frac{U}{a} = \left\{\frac{\sqrt{1+(.15L_x)^4}}{(U_j/a_\infty)^2} - \frac{\gamma-1}{2}\right\}^{-1/2} e^{-(\frac{r}{a})^n}$$

$$C = \frac{a}{a_\infty} = \left\{1+\frac{\gamma-1}{2}(\frac{U}{a})^2\right\}^{-1/2}. \qquad (18)$$

A large value for exponent n corresponds to a slug flow profile which is the the characteristic of the exit. By allowing n to gradually decrease in flow direction, one can recover a Gaussian distribution for the downstream profile. To illustrate the refraction effects, two plume models have been considered. In model one, n is constant ($n = 4$), corresponding to a top-hat shape for M. In model two, n starts from near 6 at the exit and decays to 2 at about 12 diameters from the exit according to

$$n = \frac{5b}{(X/D+.1)^{1.25}+b} + 1, \quad b = 5. \qquad (19)$$

This changes the shape of M from a top-hat to a Gaussian as the flow develops. The velocity profiles for the two models are illustrated in figure 2 for a jet spreading at $\alpha = 10^o$. The location of the exit plane is defined as the section at which the jet diameter is one. In the following numerical computations the jet exit Mach number is $U_j/a_\infty = .99$ and the source is at seven diameters from exit plane where $U_o/a_\infty = .87$ on the centerline.

Numerical Results and Discussion

The spherical directivity pattern corresponding to equation (15) can be written as

$$\overline{P^2}(\mathbf{X}) \propto (\frac{\lambda_o^3}{\lambda})(\frac{sin\,\mu}{sin\,\theta_\infty})\frac{(1-\frac{\mathbf{U_o}}{a_\infty}\cdot\mathbf{p_o})^2(1-\frac{\mathbf{U}}{a_\infty}\cdot\mathbf{p})^2}{(1-\frac{\mathbf{U_c}}{a_\infty}\cdot\mathbf{p_o})^5\,|\,\frac{\partial(\theta_\infty,\phi_\infty)}{\partial(\mu,\delta)}\,|} \qquad (20)$$

where $\mathbf{U_o}$ is the mean flow velocity at the source location and in general is different from the source convection velocity $\mathbf{U_c}$. For a parallel jet, the directivity pattern outside the zone of silence is commonly accepted to follow the Doppler factor to -3 power. For a spreading jet, this remains valid, that is $\overline{P^2} \propto (1-\mathbf{U_o}\cdot\mathbf{p_o}/a_\infty)^2/(1-\mathbf{U_c}\cdot\mathbf{p_o}/a_\infty)^5$, as long as the source is convecting along the center-axis of an axisymmetric jet.

As the source is placed off-axis, the non-axisymmetric nature of the problem creates a directivity pattern that will not follow the above simple rule; rather the source eccentricity as well as the relative azimuthal angle between the source and observer will influence the directivity pattern. However, the directivity due to a ring source, obtained from the circumferential integral of the noise produced by compact quadrupole sources distributed on the ring will be shown to, more or less, follow the Doppler factor to -3 power outside the quieting zone. Here for numerical computations, the source convection velocity is taken to be a weighted average of the mean flow velocity at the jet exit and the source location

$$\frac{\mathbf{U_c}}{a_\infty} = .5(\frac{\mathbf{U_o}}{a_\infty}) + \beta_c(\frac{\mathbf{U_j}}{a_\infty}) \qquad (21)$$

where β_c is an empirical constant. The source location at any axial section is defined through angles θ_o and ϕ_o.

To investigate the boundary of the zone of silence, the source was moved toward the centerline by changing θ_o while X/D is constant. For a ray beaming straight downstream ($\mu = 0$), the final polar angle $\theta^\star$ is plotted vs. the source location. It should be noted that in order to arrive at the boundary of the zone of silence, emission at nonzero values of μ should also be considered. When a ray is emitted towards the axis ($\mu \neq 0$), a complete refraction can result in propagation of noise to shallower angles than those defined through ($\mu = 0$). However, subsequent ray-tracing shows that for high speed jets, there is little difference between the two results. This difference disappears as the source approaches the centerline.

Figure 3(a), corresponding to model one, shows how the zone of silence (defined through angle $\theta^\star$) can be eliminated by allowing a small jet spreading angle. For model two, however, figure 3(b) shows that the zone of silence is still present even at spreading angles as large as $\alpha = 20°$. This comparison clearly demonstrates the significance of velocity gradients in bending the rays away from the center axis. Rays that are emitted near the centerline should travel a relatively longer distance before they get refracted and as a result they run into high gradient regions of the plume (similar to the Gaussian profile in model two) and a zone of silence is formed. Another significant observation that can be made here is related to what is termed the "quieting zone". As the source moves away from the center, there are rays emitted on a cone of emission with $\mu > 0$ that can go through complete refraction and reach values of θ_∞ smaller than $\theta^\star$. Therefore one can conclude that within the zone of silence, the sound pressure level (SPL) does not drop to zero at once; rather there is a gradual decay in noise level. As the jet spreading angle approaches zero, the size of the zone of silence in both 3(a) and 3(b) approach the parallel flow solution given as

$$\theta^\star \; < \; cos^{-1} \frac{1}{C_o(1+M_o)} \qquad (22)$$

where $C_o = .92$ and $M_o = .94$ at $X/D = 7$.

In all remaining discussions the jet spreading angle is held at $\alpha = 10°$ and the convection velocity follows equation (21) with $\beta_c = .3$. For a source on the axis, the sound field is axisymmetric and results similar to those given in [19] are found. In figure 4 the slope of the curve within the quieting zone will in general be sensitive to the jet spreading angle. To compare the present prediction with data, Stone's correlation [26] was employed. The directivity pattern $\overline{P^2}(1-M_c\, cos\,\theta)^3$ obtained from these correlations is identically equal to one outside the quieting zone; within the quieting zone the slope gradually increases with frequency. For a Helmholtz number of $He = fD/a_\infty = 31.6$, the data correlation shows a slope of 19° per octave compared with 10.5° per octave calculated from the high frequency geometrical theory. As we shall demonstrate later on, by using a ring source, this difference in slopes narrows down substantially. In applying Stone's correlation, the convection Mach number for the source was substituted according to equation (21).

When the source is placed off-axis, the numerical work in solving the propagation equations is greatly increased. In general an iteration process should be applied to find a ray that propagates through a specified observer location. Figure 5(a) shows the variation in the shielding effect as a function of source eccentricity. The source is placed at three locations defined through $\theta_o = (0, 2°, 5°)$ with $\phi_o = 0$ and $X/D = 7$ while the azimuthal angle for the observer is held at $\phi_\infty = 0$. Notice that as the source is brought closer to the observer, the shielding effect of the mean flow decreases in downstream directions resulting in an increase in SPL while an opposite effect is observed upstream. According to figure 5(b), as the source move further away from the axis, the SPL does not scale with power -3 of the Doppler factor.

Of particular interest is the spherical directivity of an off-axis convecting quadrupole. This is demonstrated in figures 6 and 7 for a source at $\theta_o = 5°$ and $\phi_o = 0$. The polar directivity at constant ϕ_∞ is given figure 6 while the corresponding azimuthal directivity is plotted in figure 7 for a range of the parameter θ_∞. In general one can observe an increase in azimuthal variation of sound further downstream. For $\theta_\infty > 110°$, an increase in SPL is predicted as the observer moves azimuthally to the opposite side of the source. In fact if the computation is carried out for $\phi_\infty > 160°$, a singularity starts to develop at $\phi_\infty \rightarrow 180°$ and $\theta_\infty \rightarrow 141°$ as the Jacobian in equation (20) approaches zero (see figure 8). This indicates a reduction in ray tube area resulting in focusing or concentration of rays in a neighbourhood which is the caustics of geometrical acoustics. The sound field obtained according to equation (13) is essentially the first term in asymptotic expansion in inverse powers of wave number. As was pointed out by J. Keller [20, 27], the zero-order term in this expansion can become infinite even when the field is perfectly regular.

A uniform asymptotic expansion at the caustics for a still medium was suggested by Ludwig [21] in terms of the Airy function and its derivatives. A more rigorous analysis was suggested by Zauderer [22] by looking into the modified forms of asymptotic expansions of the reduced wave equation in transition regions. One might expect similar expansions for the case of a moving medium. No attempt has been made here to replace equation (13) with a solution uniformly valid near the

caustic; rather a simple extrapolation of the solution given in figure 7 was applied to predict the field at $180° \geq \phi_\infty \geq 160°$. Assuming that a ring source is obtained from the superposition of independent correlation volume elements distributed around the center axis, for an axisymmetric jet one can simply integrate the area under each curve in figure 7 and compute the sound field due to a convecting ring source. This idea can further be extended to an entire jet by subdividing the plume into axial slices that are formed from ring elements.

The most important result of the present theoretical prediction is summarized in figures 9, 10 and 11. The noise directivity for a ring source is shown in figure 9. The presence of a caustic manifests itself as a change in slope around 120 degrees. Such a change in slope can also be observed in most experimental reports on the directivity of jet mixing noise [26]. Figure 10 presents the Doppler factor as calculated from the ray theory normalized with respect to the conventional definition based on the line-of-sight method. Each curve represents the change in the Doppler factor as the source is allowed to navigate on a ring relative to a fixed observer at θ_∞. This can clearly be attributed to the required change in the initial direction of the ray as a function of source location. Finally, the scaling of directivity with power -3 of the Doppler factor is investigated in figure 11. Within the quieting zone, the prediction gives a slope of 17° per octave compared with 19.3° per octave computed from Stone's correlation with a Helmholtz number of 31.6. This is a significant improvement over the earlier comparisons for a point source. It should also be noted that even at a Helmholtz number of 10, the data correlations give a slope of 23° per octave, not too far from our high frequency prediction.

Concluding Remarks

It was shown, through a relatively simple jet model, that geometric acoustics can be employed to study the propagation of high frequency jet noise. Based on the model jets considered here, it has been demonstrated that a zone of silence is formed near the downstream jet axis. The size of the zone of silence can vary with source location. Further it was shown that ray focusing results in formation of a caustic upstream and azimuthally on the opposite side of the source. Ray acoustics is a particularly powerful tool in investigating noise directivity of non-axisymmetric jets. These computations can easily be extended to supersonic jets. For a supersonic jet, the maximum value for the semiangle of cone of emission of a source should decrease with increasing the mean flow Mach number. Finally, further improvements that need to be considered are:

(1) the effect of source anisotropy can be studied by replacing Q with $Q_{ij}p_ip_j/|\mathbf{p}|^2$ in equation (15);
(2) the Doppler factor as defined in this analysis should further be investigated for supersonic jets where the conventional definition becomes singular at $\theta_\infty = cos^{-1}1/M_c$.

Acknowledgements

The authors would like to thank M. E. Goldstein of NASA Lewis Research Center for suggesting the high frequency problem of geometrical acoustics.

References

1. Lighthill, M. J., "Sound generated aerodynamically," *Proc. Roy. Soc.*, **A267**, 1962, 147-182.
2. Ffowcs Williams, J. E., "The noise from turbulence convected at high speed," *Phil. Trans. Roy. Soc.*, **A255**, 1963, 469-503.
3. Lighthill, M. J., "The fourth annual fairey lecture: the propagation of sound through moving fluids," *J. Sound Vib.*, **24(4)**, 1972, 471-479.
4. Tester, B. J. & Morfey, C. L., "Developments in jet noise modeling - theoretical predictions and comparisons with measured data," *J. Sound Vib.*, **46(1)**, 1976, 79-103.
5. Balsa, T. F., "The far field of high frequency convected singularities in sheared flows, with application to jet-noise prediction," *J. Fluid Mech.*, **74**, 1976, 193-208.
6. Scott, J. N., "Propagation of sound waves through linear shear layer," *AIAA Journal*, **17**, 1979, 237-244.
7. Gliebe, P. R. & Balsa, T. F., "The aerodynamics and acoustics of coaxial jet noise," AIAA paper 76-492., 76.
8. Goldstein, M. E., "The low frequency sound from multipole sources in axisymmetric shear flows," *J. Fluid Mech.*, **70**, 1975, 595-604.
9. Balsa, T. F., "The acoustic field of sources in shear flow with application to jet noise: convective amplification," *J. Fluid Mech.*, **79**, 1977, 33-47.
10. Goldstein, M. E., "The low frequency sound from multipole sources in axisymmetric shear flows - part II," *J. Fluid Mech.*, **75**, 1976, 17-28.
11. Goldstein, M. E., *Aeroacoustics*, McGraw-Hill, 1976.

12. Mani, R., Gliebe, P. R., Balsa, T. F. et al, "High velocity jet noise source location and reduction," Task 2, FAA-RD-76-79-II, 1978.

13. Khavaran, A., Krejsa, E. A. & Kim, C. M., "Computation of supersonic jet mixing noise for an axisymmetric CD nozzle using $k\epsilon$ turbulence model," AIAA paper 92-0500, 1992.

14. Schubert, L. K., "Numerical study of sound refraction by a jet flow. I. Ray acoustics," *J. Acoust. Soc. Am.*, **51**, 1972, 439-446.

15. Schubert, L. K., "Numerical study of sound refraction by a jet flow. II. Wave acoustics," *J. Acoust. Soc. Am.*, **51**, 1972, 447-463.

16. Goldstein, M. E., "High frequency sound emission from moving point multipole sources embedded in arbitrary transversely sheared mean flows," *J. Sound Vib.*, **80(4)**, 1982, 499-522.

17. Avila, G. S. S. & Keller, J. B., "The high frequency asymptotic field of a point source in an inhomogeneous medium," *Commun. Pure Appl. Math.*, **16**, 1963, 363-381.

18. Durbin, P. A., "High frequency Green function for aerodynamic noise in moving media, part I: general theory," *J. Sound Vib.*, **91(4)**, 1983, 519-525.

19. Durbin, P. A., "High frequency Green function for aerodynamic noise in moving media, part II: noise from a spreading jet," *J. Sound Vib.*, **91(4)**, 1983, 527-538.

20. Kay, I. & Keller, J. B., "Asymptotic evaluation of the field at a caustic," *J. Appl. Phys.*, **25**, 1954, 876-883.

21. Ludwig, D., "Uniform asymptotic expansions at a caustic," *Commun. Pure Appl. Math.*, **19**, 1966, 215-250.

22. Zauderer, E., "Uniform asymptotic solutions of the reduced wave equation," *J. Math. Analysis Appl.*, **30**, 1970, 157-171.

23. Jones, D. S., "The mathematical theory of noise shielding," *Progress in Aerospace Science* **17**, 1977, 149-229.

24. Candel, S. M., "Numerical solution of conservation equations arising in linear wave theory: application to aeroacoustics," *J. Fluid Mech.* **83**, 1977, 465-493.

25. Groesbeck, D. E., Huff, R. G., & von Glahan, U. H., "Comparison of jet Mach number decay data with a correlation and jet spreading contours for a large variety of nozzles," NASA TN D-8423, 1977.

26. Stone, J. R., Groesbeck, D. E., & Zola, C. L., "An improved prediction method for noise generated by conventional profile coaxial jets," AIAA paper 81-1991, 1981.

27. Keller, J. B., *Geometrical Theory of Diffraction, Calculus of Variations and its Applications, Proc. Symposia Appl. Math.*, **8**, 1958, 27-52, McGraw-Hill, NY.

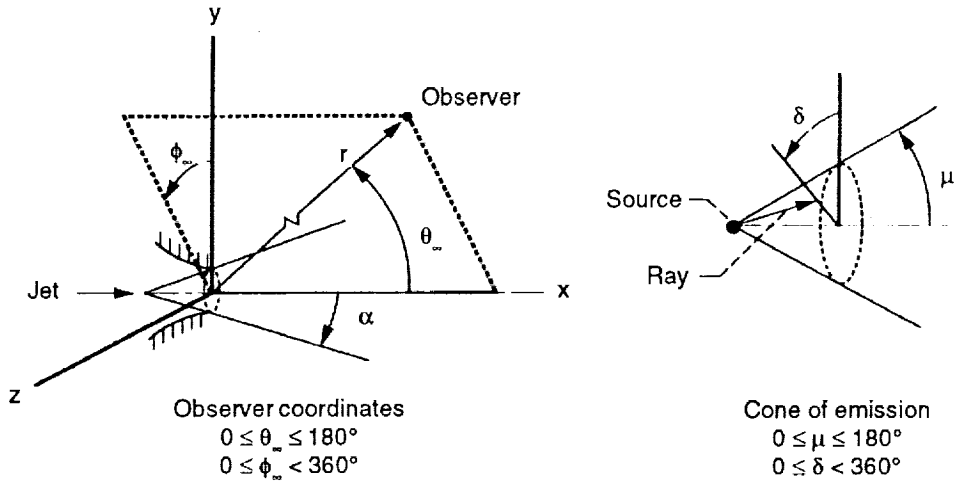

Figure 1. Source and observer coordinates.

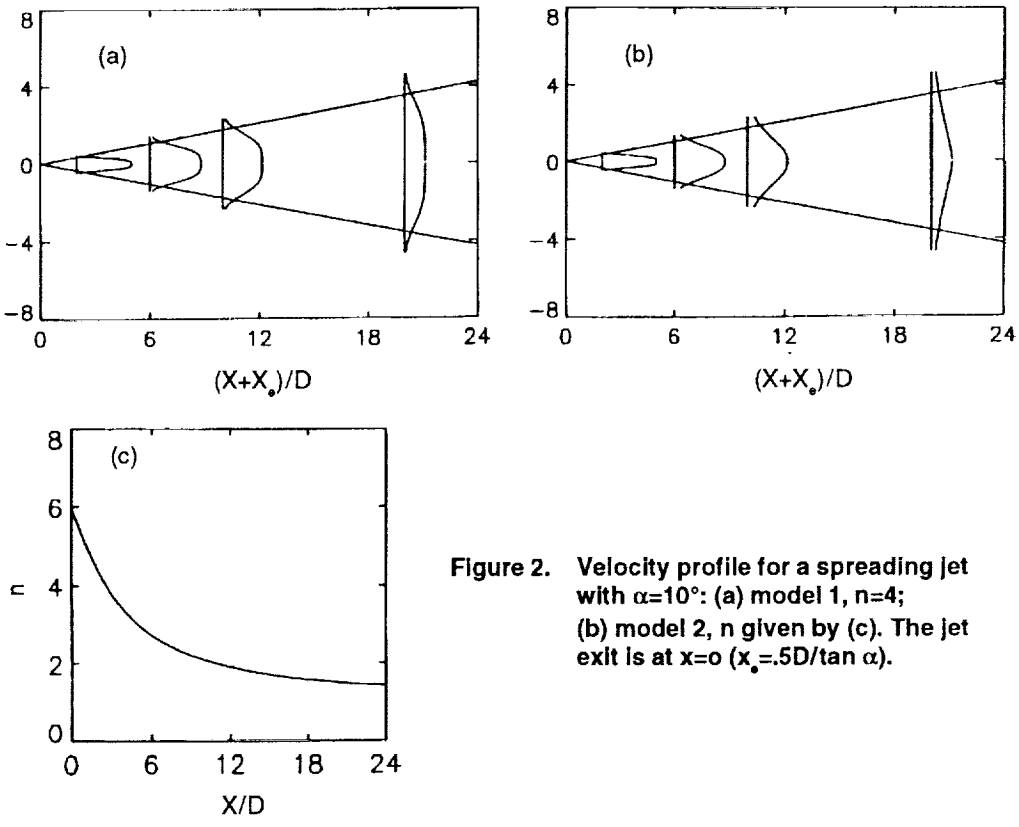

Figure 2. Velocity profile for a spreading jet with α=10°: (a) model 1, n=4; (b) model 2, n given by (c). The jet exit is at x=o (x_o=.5D/tan α).

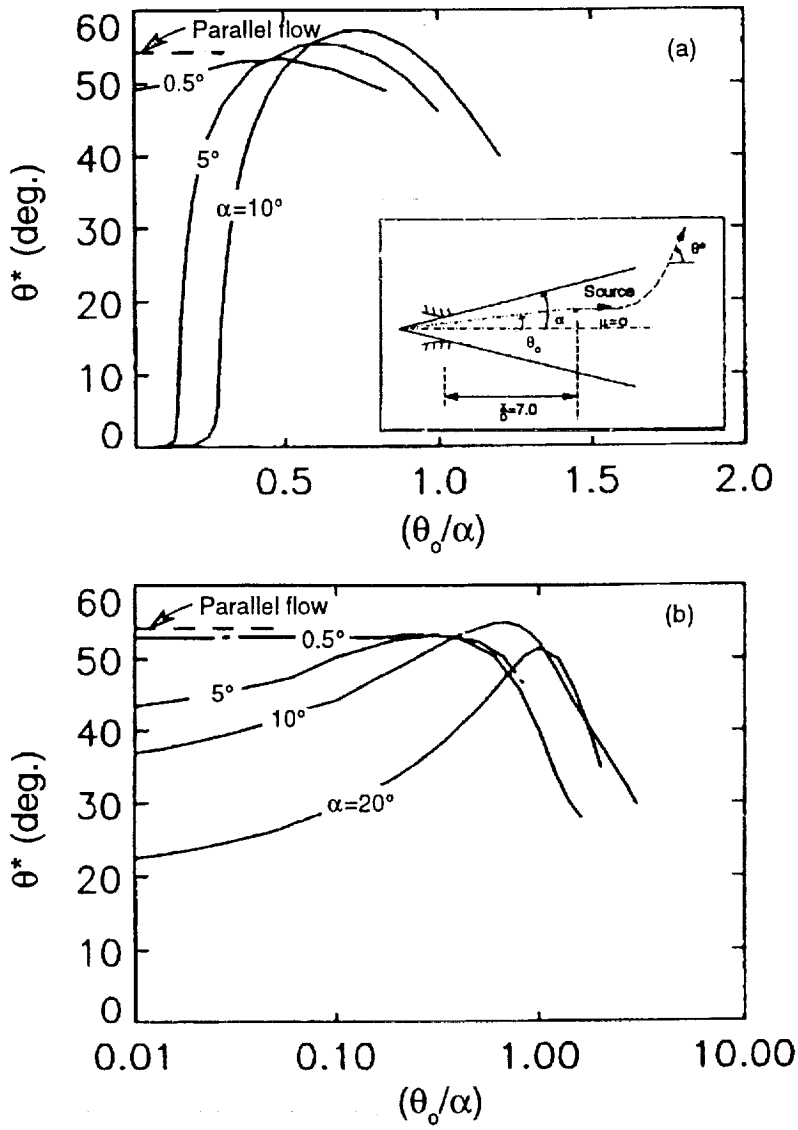

Figure 3. Boundary of zone of silence for a source at x/D=7. (a) Model 1; (b) Model 2. The jet spreading angle α is indicated as a parameter.

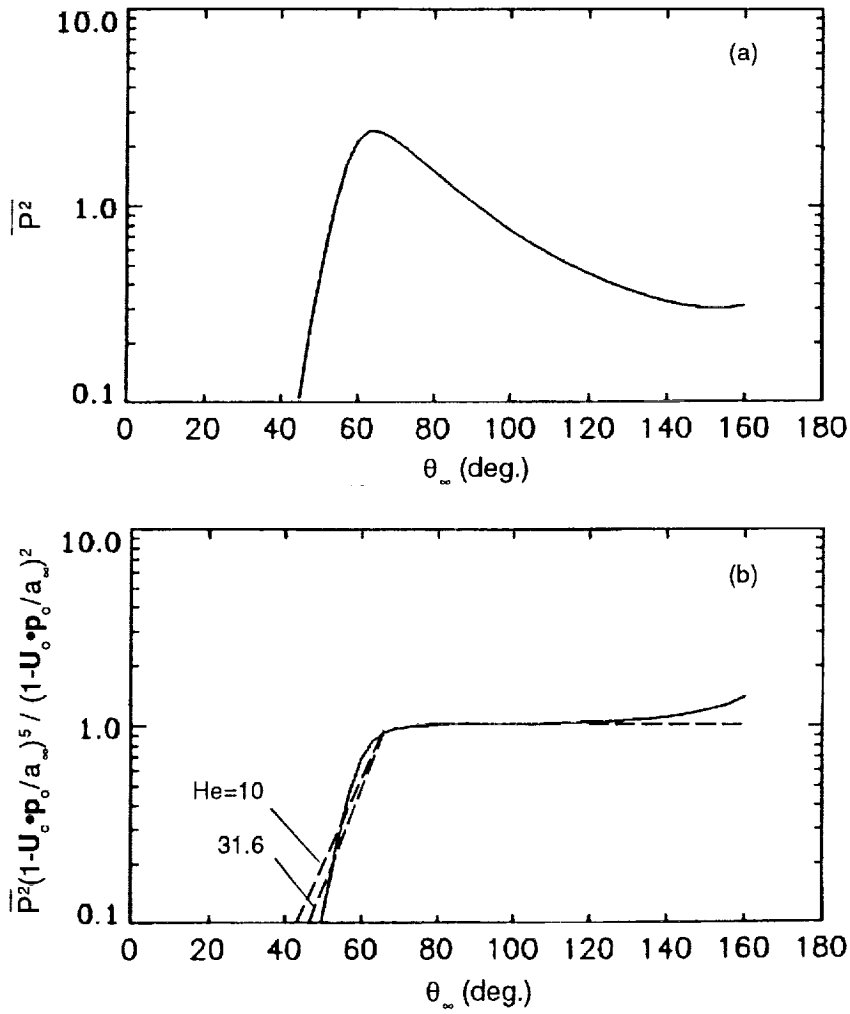

Figure 4. Noise directivity for a source convecting along the center axis at X/D=7 for α=10° using model 2. In 4(b) (—) is the high frequency computation and (– –) is $\overline{P^2}(1-U_c \cos \theta_\infty/a_\infty)^3$ obtained from data [26] for indicated Helmholtz numbers.

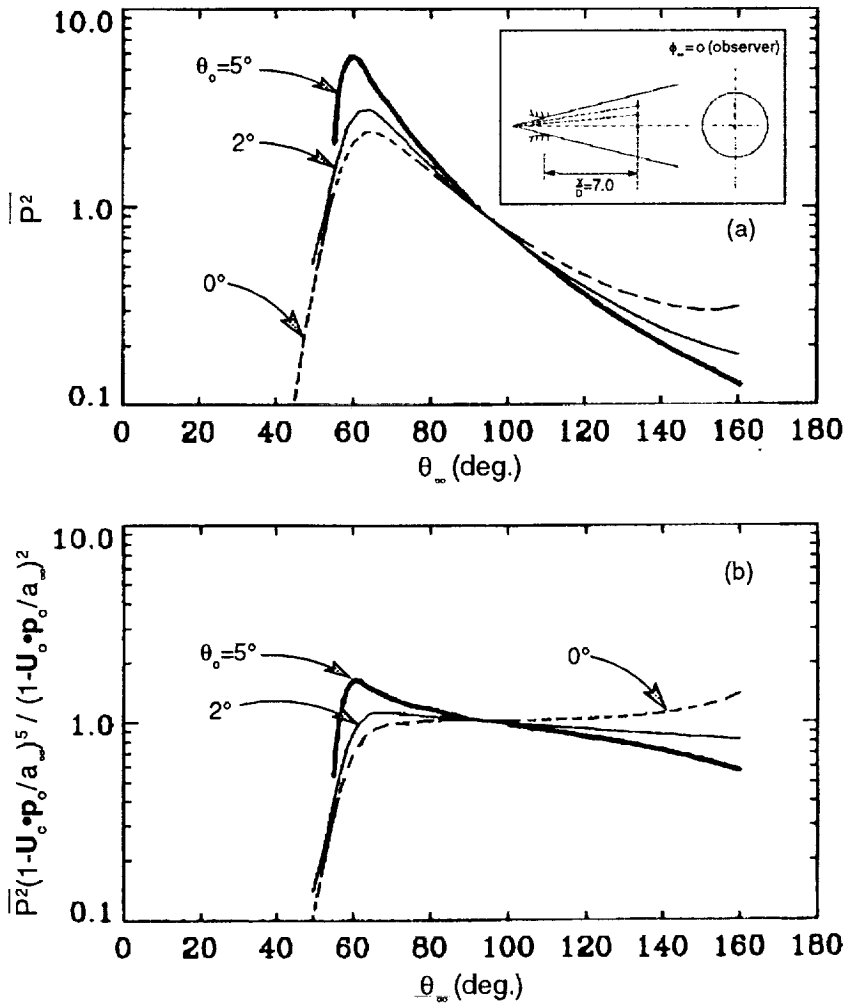

Figure 5. The effect of source location on directivity pattern; the sources are at X/D=7, ϕ_o=0° and θ_o=0°, 2° and 5°. The observer is at ϕ_-=0°.

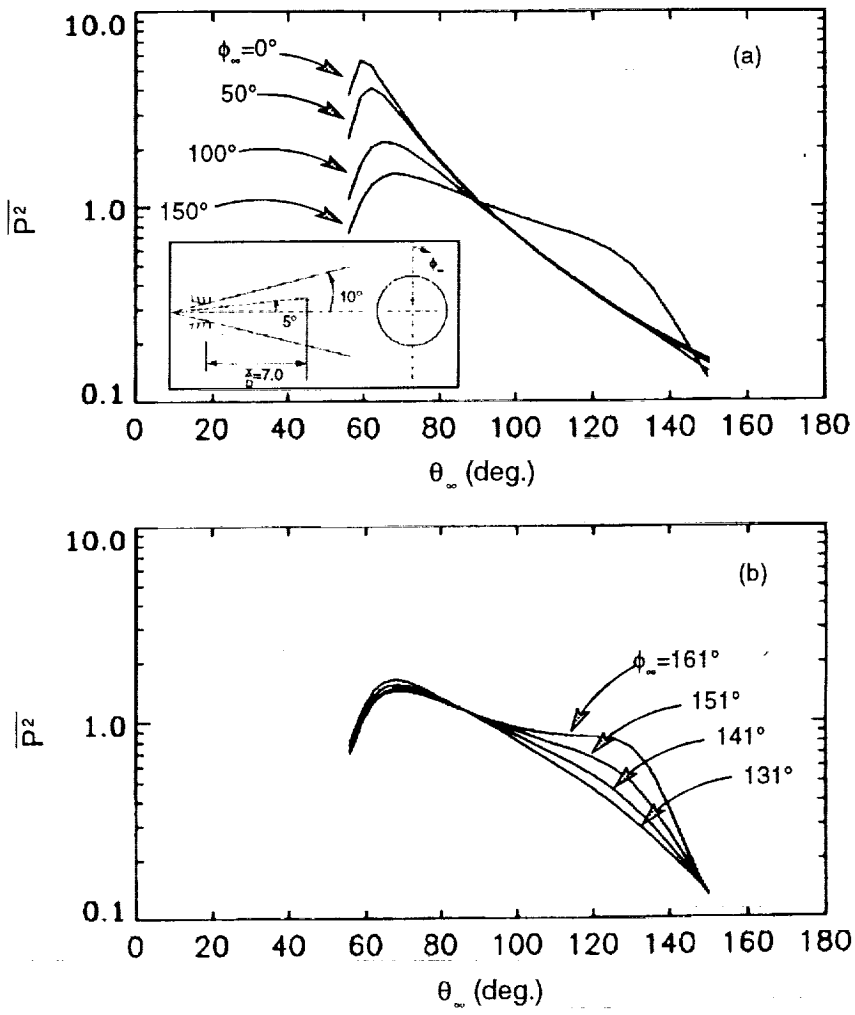

Figure 6. Spherical directivity pattern for an off-axis source. The source is located at X/D=7, ϕ_o=0 and θ_o=5°. The formation of singularity near the caustic is demonstrated in 6(b).

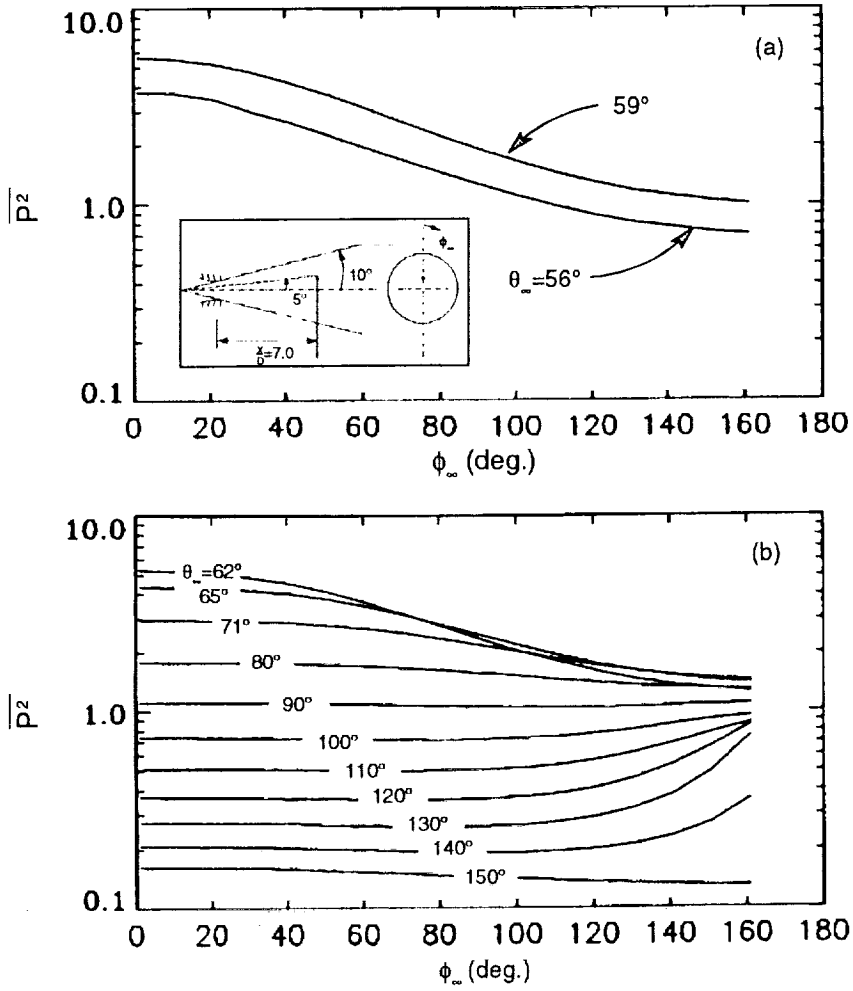

Figure 7. Spherical directivity vs the azimuthal observation angle (polar angle is indicated as a parameter). The source location is the same as Figure 6. Figure 7(a) shows the sharp drop in noise level within the quieting zone.

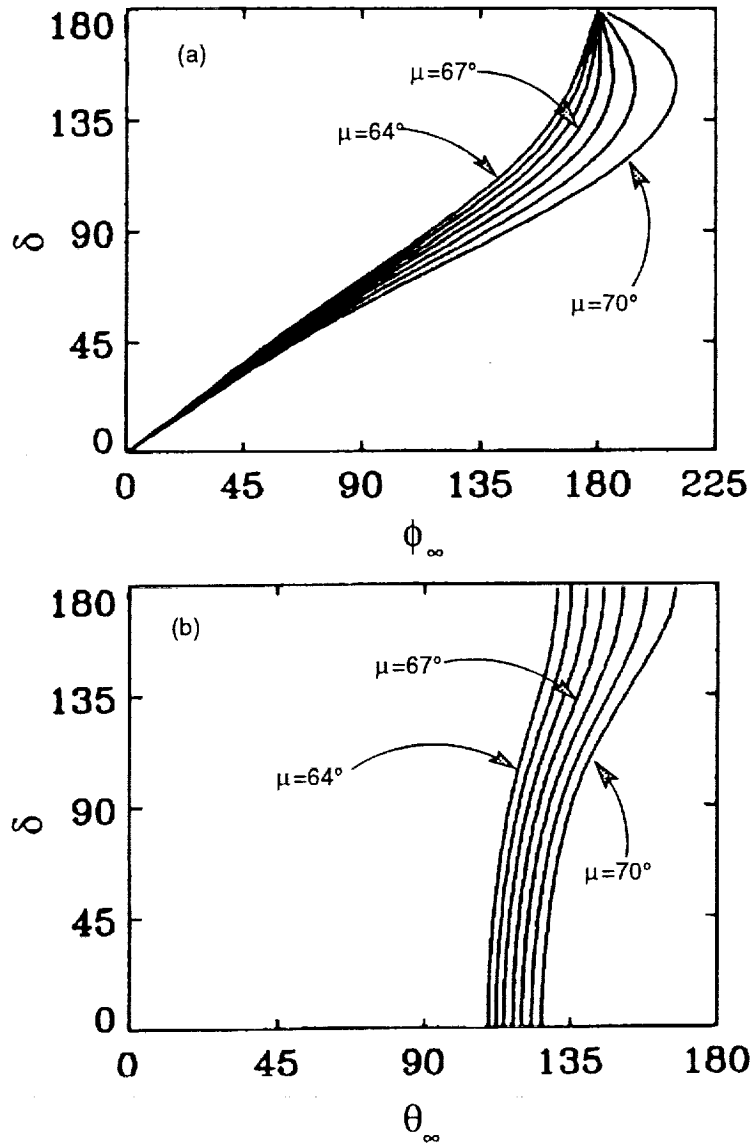

Figure 8. Ray-tracing showing the reduction in the area of ray tube in the neighborhood of μ=67°. This results in a caustic at $\theta_{-} \rightarrow 141°$ and $\phi_{-} \rightarrow 180°$.

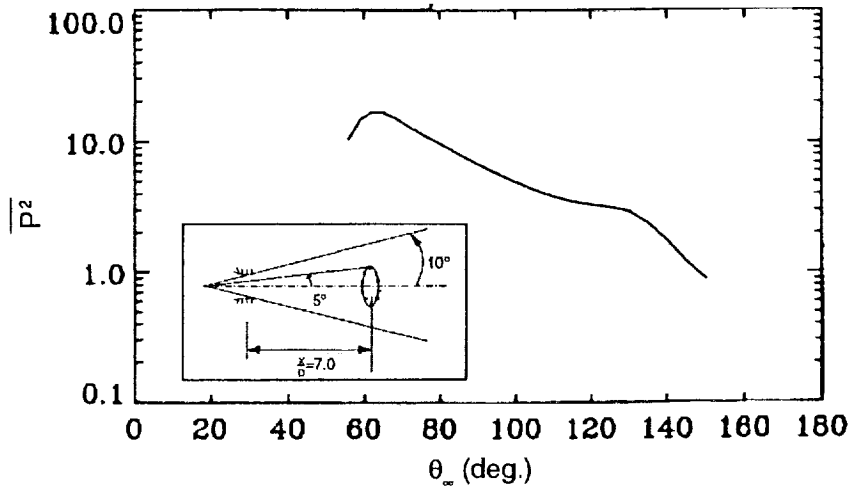

Figure 9. Directivity pattern for a ring source.

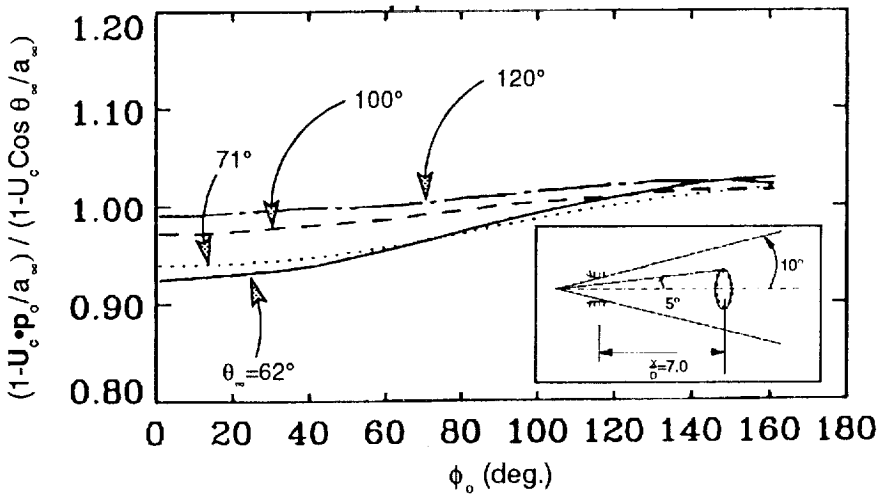

Figure 10. Variations in the Doppler effect due to change in source location. The observer is fixed at ϕ_∞=0; while the source moves on a ring.

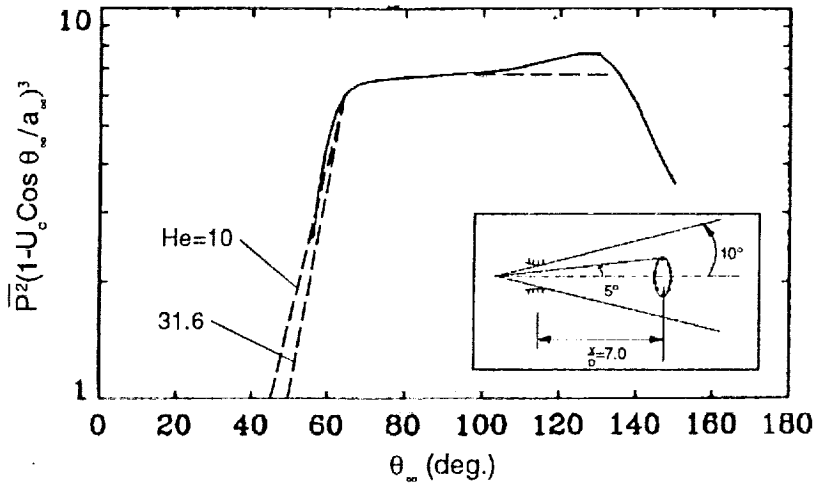

Figure 11. Comparison between data [26] and high frequency approximation. The solid line (—) is the computation for a ring source. The data correlation is given as (– –) for indicated Helmholtz numbers.

REPORT DOCUMENTATION PAGE

Form Approved
OMB No. 0704-0188

1. AGENCY USE ONLY (Leave blank)	2. REPORT DATE	3. REPORT TYPE AND DATES COVERED
	January 1993	Technical Memorandum

4. TITLE AND SUBTITLE
Propagation of High Frequency Jet Noise Using Geometric Acoustics

5. FUNDING NUMBERS
WU-537-02-23

6. AUTHOR(S)
A. Khavaran and E.A. Krejsa

7. PERFORMING ORGANIZATION NAME(S) AND ADDRESS(ES)
National Aeronautics and Space Administration
Lewis Research Center
Cleveland, Ohio 44135-3191

8. PERFORMING ORGANIZATION REPORT NUMBER
E-7471

9. SPONSORING/MONITORING AGENCY NAMES(S) AND ADDRESS(ES)
National Aeronautics and Space Administration
Washington, D.C. 20546-0001

10. SPONSORING/MONITORING AGENCY REPORT NUMBER
NASA TM-106013

11. SUPPLEMENTARY NOTES
Prepared for the 31st Aerospace Sciences Meeting and Exhibit sponsored by the American Institute of Aeronautics and Astronautics, Reno, Nevada, January 11-14, 1993. A. Khavaran, Sverdrup Technology, Inc., Lewis Research Center Group, 2001 Aerospace Parkway, Brook Park, Ohio 44142 and E.A. Krejsa, NASA Lewis Research Center. Responsible person, A. Khavaran, (216) 891-2293.

12a. DISTRIBUTION/AVAILABILITY STATEMENT
Unclassified - Unlimited
Subject Category 71

12b. DISTRIBUTION CODE

13. ABSTRACT *(Maximum 200 words)*

Spherical directivity of noise radiated from a convecting quadrupole source embedded in an arbitrary spreading jet is obtained by ray-tracing methods of geometrical acoustics. The six propagation equations are solved in their general form in a rectangular coordinate system. The noise directivity in the far field is calculated by applying an iteration scheme that finds the required radiation angles at the source resulting in propagation through a given observer point. Factors influencing the zone of silence are investigated. The caustics of geometrical acoustics and the exact location where it forms is demonstrated by studying the variation in ray tube area obtained from transport equation. For a ring source convecting along the center-axis of an axisymmetric jet, the polar directivity of the radiated noise is obtained by an integration with respect to azimuthal directivity of compact quadrupole sources distributed on the ring. The Doppler factor is shown to vary slightly from point to point on the ring. Finally the scaling of the directivity pattern with power -3 of Doppler factor is investigated and compared with experimental data.

14. SUBJECT TERMS
Jet noise; Acoustics; Sound propagation; Geometric acoustics

15. NUMBER OF PAGES
18

16. PRICE CODE
A03

17. SECURITY CLASSIFICATION OF REPORT	18. SECURITY CLASSIFICATION OF THIS PAGE	19. SECURITY CLASSIFICATION OF ABSTRACT	20. LIMITATION OF ABSTRACT
Unclassified	Unclassified	Unclassified	